Estuarine, Coastal and Shelf Science 183 (2016) 213–220

Contents lists available at ScienceDirect

Estuarine, Coastal and Shelf Science

journal homepage: www.elsevier.com/locate/ecss

Estimation of seasonal topographic variation in tidal flats using waterline method: A case study in Gomso and Hampyeong Bay, South Korea

Zhen Xu [a, c], Duk-jin Kim [a, *], Seung Hee Kim [a], Yang-Ki Cho [a], Sun-Gu Lee [b]

[a] School of Earth and Environmental Sciences, Seoul National University, Seoul 151-742, South Korea
[b] Korea Aerospace Research Institute, Daejeon 305-333, South Korea
[c] Department of Geography, Yanbian University, Yanji 133002, China

ARTICLE INFO

Article history:
Received 16 May 2016
Received in revised form
25 August 2016
Accepted 18 October 2016
Available online 21 October 2016

Keywords:
Seasonal variation
Waterline method
Tidal flat
Topographic changes

ABSTRACT

Morphologic and topographic changes of tidal flats can be key indicators for monitoring environmental changes and sea level rise. Recently, a number of studies have been performed to estimate temporal topographic changes in tidal flats based on the waterline method using a number of remote sensing data that were acquired at different tidal heights. However, the effect of seasonal variation has not been taken into consideration, nor been understood so far. In this study, 18 scenes of Landsat TM and ETM+ data, covering the period 2003–2004, and corresponding tidal gauge observation data, were used to estimate seasonal topographic variations in two major tidal flats in Gomso and Hampyeong Bay in the southern part of the west sea of South Korea, using the waterline method. Our results showed that the summer deposition was dominant in Gomso Bay with overall average seasonal topographic increase of approximately 18.6 cm. In contrast, Hampyeong Bay showed more dominant summer erosion with overall average seasonal topographic subsidence of about 5.0 cm. In addition, the net overall sedimentation budget was estimated as 6,308,047 m^3 and -2,210,986 m^3 in Gomso and Hampyeong Bay, respectively. The results also indicates that although both bays of Gomso and Hampyeong are classified as semi-enclosed tidal flat, the sedimentary facies caused by formation geometry and sediment type led to different topographic changes. The results demonstrate that the amount of seasonal topographic variations is not negligible and are expected to improve the accuracy of topographic change derived by the waterline method.

1. Introduction

Tidal flats are considered as an important coastal geomorphologic system, which provide habitats for wildlife, resources for land reclamation and coastal protection against extreme storm events (Allen, 2000; Allen and Pye, 1992; Wang et al., 1999). Thus, morphologic or topographic changes in tidal flats or intertidal areas, have attracted worldwide interest (Van Stokkom et al., 1993; Welch et al., 1992). The western coast of the Korean Peninsula is famous for its large tidal range (up to 9 m) and vast tidal flats (Yoo et al., 2005). Frequent monitoring is required to protect this valuable and vulnerable ecological system, endangered by shipping, fishery and coastal reclamation project. However, morphologic or topographic changes in tidal flats are difficult to estimate due to their poor accessibility, short exposure, and lack of suitable transportation (Ryu et al., 2008). Furthermore, it is difficult to retrieve the tidal flat topography of the past few years or even decades using ground surveys, ship-based echo-sounding, or airborne stereophotogrammetry (Klemas, 2011; Mason et al., 2000; Sallenger et al., 2003; Wimmer et al., 2000). Nevertheless, specific applications of high precision mapping have been pursued in some countries, using airborne-based light detection and ranging (LiDAR) and synthetic aperture radar (SAR) (Deronde et al., 2006; Gade et al., 2008; Green et al., 1996; Greidanus et al., 1999; Stockdonf et al., 2002; Wimmer et al., 2000; Gade et al., 2014). These methods are also limited to apply changes of continental scales, due to the rapidly changing tidal conditions and huge cost involved in airborne data acquisitions (Cracknell, 1999; Ryu et al., 2008). In

* Corresponding author.
E-mail address: djkim@snu.ac.kr (D.-j. Kim).

http://dx.doi.org/10.1016/j.ecss.2016.10.026

spite of being relatively more sophisticated, the waterline method using satellite images embodies an effective alternative to monitor and detect topographic changes occurring over the large area of tidal flats (Ahn et al., 1989; Heygster et al., 2010; Hoja et al., 2000; Mason et al., 1995; Ryu, 2003; Zhao et al., 2008). Recently, intensive research has been conducted on the detection and estimation of temporal topographic changes in the tidal flat using the waterline method, based on various remote sensing data. Chen and Rau (1998) computed a Digital Elevation Model (DEM) in Taiwan using waterlines recorded by SPOT satellite images, to estimate coast erosion. Ryu et al. (2008) carried out a quantitative assessment of the morphologic changes affecting the tidal flats of Gomso Bay, Korea, using the waterline method coupled with a series of satellite images and ground truth data. Choi et al. (2011) examined the topographical control of surface sedimentary facies distribution in the Southern Ganghwa tidal flat, South Korea, by employing the intertidal DEM generated by the waterline method with Landsat Enhanced Thematic Mapper Plus (ETM+) images, combined with GIS analysis. Lee et al. (2011) analyzed the anthropogenic-related changes in local sedimentation trends and morphology, using the waterline method in the Ganghwa tidal flat, South Korea. The quantitative analysis of the relationship between the accuracy of tidal flat DEM was performed, based on the waterline method and the factors that influences the DEMs in a case study of the Dongsha Sandbank (Liu et al., 2013). Li et al. (2014) generated the annual topographic maps using the waterline method based on the SAR image in the northern parts of the German Wadden Sea for the years 1996–1999 and 2006–2009, and performed quantitatively estimation and monitors the development of the tidal flats.

Although these researches have applied waterline method using remote sensing data to detect topographic changes in tidal flats, the effect of seasonal topographic variation was not considered while monitoring such topographic changes. In this study, the amounts of seasonal topographic variations are quantitatively assessed by applying the waterline method, using satellite images acquired in short time span and different seasons.

2. Materials and methods

2.1. Study area

The study area is located in the southwestern coast of the Korean Peninsula, where two major tidal flats reside in Gomso Bay and Hampyeong Bay. Tidal flats in Gomso and Hampyeong Bay are classified as semi-enclosed coast tidal flat. The climate in the study area is typically characterized by hot humid summers with weak southerly winds and cool dry winters with strong winds from north under the influence of Asian monsoon. Furthermore, the seasonal precipitation pattern involves heavy rainfall during summer and the tides are primarily semi-diurnal.

Gomso Bay, a 7–9 km wide and 20 km long funnel-shaped embayment, is located in the northern part of the study area as shown in the upper part of Fig. 1. The main tidal channel runs parallel to the northern coast, losing its identity at the bay-mouth area. The tidal flats, extending some 3–5 km, are broadly developed along the southern shoreline of the bay, with an average slope of 0.09° (Chang and Choi, 2001). The main tidal channel, with depths up to 20 m, runs west-east in the northern section of the bay, its branch meeting Jujin Stream in the southern region of the shoreline. The mean tidal range in this area is 4.34 m, with spring and neap tide as 5.90 and 2.78 m, respectively. The maximum tidal current velocities in the main channel are 1.2 and 1.5 ms^{-1} during flood and ebb, respectively (Chang and Choi, 1998).

Hampyeong Bay is extended from northwest–southeast, with 8.5 and 17 km of maximum width and length, respectively, in the southern part of the study area (Fig. 1). The mouth of this Bay is deep and narrow, with a maximum depth of about 23 m, and a width of 1.5 km (Ryu, 2003). A large area of tidal flats has been developing along the side of the Bay, characterized by small sand bars and cheniers (Ryu, 2003). The mean tidal range in this region is 3.46 m, with mean neap and spring tidal ranges of 2.37 and 4.55 m, respectively (Waska and Kim, 2010). No rivers flow into the Bay, and the groundwater discharge runoff in the intertidal area is large enough to form small streams, causing thriving microphytobenthos communities (Waska and Kim, 2010).

2.2. Satellite images and tidal height data

Landsat TM and ETM+ data, acquired during summer (June to September) and winter (December to February) seasons, were used in our investigation. In order to estimate the seasonal variation in the tidal flats using the waterline method, a method for selecting appropriate Landsat images has been devised to extract the ones influenced by the seasonal changes. However, it is hard to distinguish seasonal effect from all of the effects because the coastal environmental is a complicated system. Nevertheless, the waterline is greatly influenced by the extremely climates, such as typhoons and storms. Therefore, we selected the no-typhoon-effect period (2003–2004) based on the historical typhoon path record data (form National Typhoon Center, Korea) to find suitable Landsat data. A total of 18 scenes with low-cloud effect were collected between 2003 and 2004 as listed in Table 1. For each bay, 9 Landsat TM or ETM+ satellite scenes, 4 in winter and 5 in summer, were selectively collected. In order to obtain short timespan waterline profiles, it is crucial to collect as short period as possible for remote sensing data. For this reason, only one Landsat TM scene which was acquired in September was included unavoidably. All of the acquired images were geometrically corrected, rectified to the world geodetic survey 1984 (WGS84) datum and projected on the Universal Transverse Mercator (UTM) coordinate system.

The tidal heights used in this study are being recorded regularly by a tidal gauge at Wido and Yeonggwang station respectively located at 35°37′5″ N, 126°18′6″ E and 35°25′34″ N, 126°25′13″ E (shown as stars in Fig. 1). The stations are operated by the Korea Hydrographic and Oceanographic Administration (KHOA), recording tidal level at 1 min interval starting from November, 2001 to present, using a floating gauge. Tide ratios and mean sea levels were used to compensate for tide differences due to distances between the nearest tidal gauge station and Gomso or Hampyeong Bays on the basis of Eq. (1). Corrected tidal height information is listed in Table 1 matching the acquisition times of acquired satellite images in each bay.

$$\textit{Corrected tidal height} = (Z - Z_0)\cdot R + S_0 \quad (1)$$

where, Z and Z_0 are recorded tidal height and mean sea level in the standard port (ex. Standard port of Gomso Bay is Wido tidal gauge station, and standard port of Hampyeong Bay is Yeonggwang tidal gauge station), R is tide ratio and S_0 is mean sea level in the any place where is Gomso or Hampyeong bay. The Z_0, R, and S_0 are reported by KHOA.

2.3. Method

In order to quantitatively estimate seasonal topographic variation in the tidal flat, waterline method is used to construct a topographic map. The term ‘waterline’ is defined as the boundary between water body and exposed tidal flat, recognizable in a remotely sensed image (Mason et al., 1997). Assuming that the waterline is a line of equal elevation, one can generate an intertidal

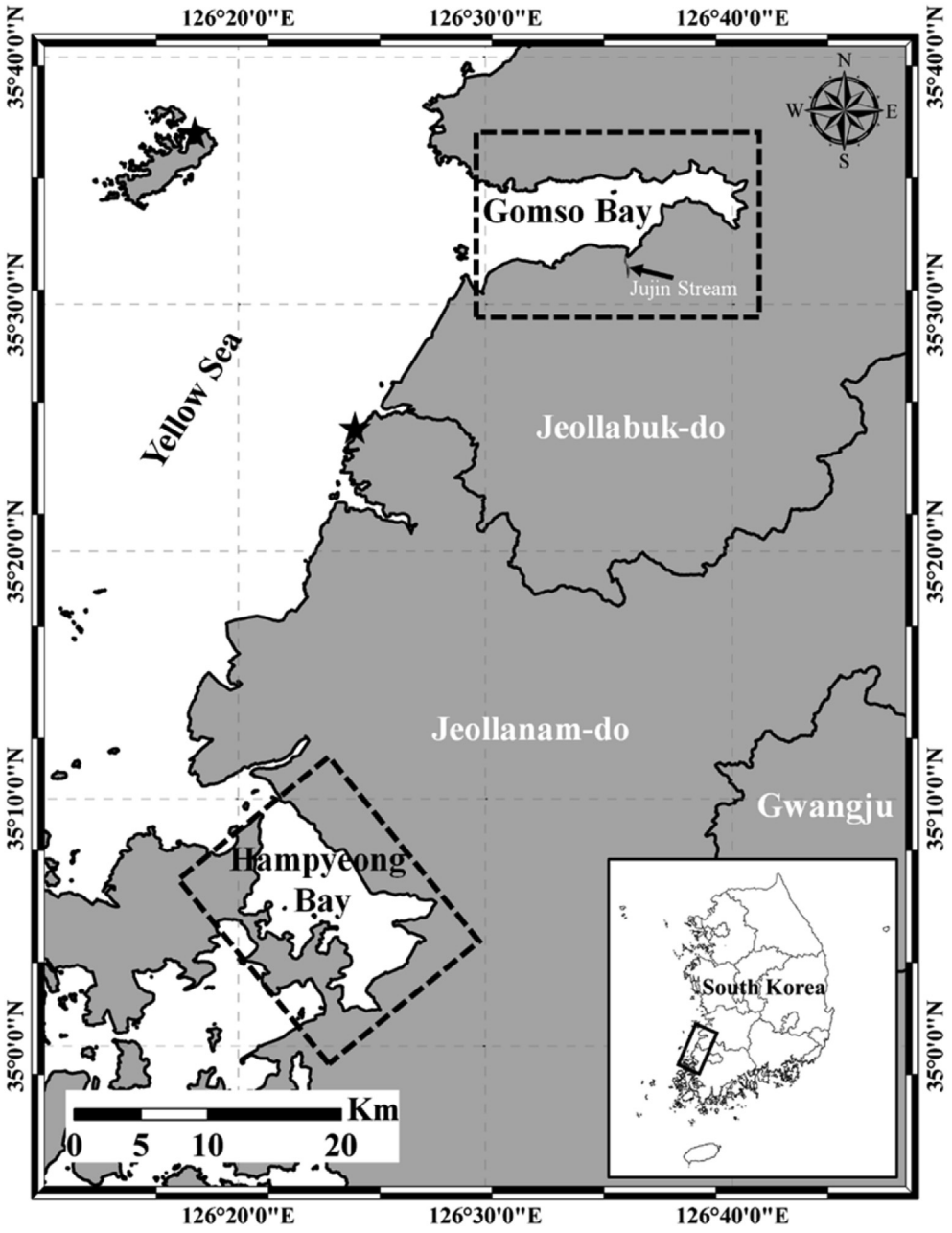

Fig. 1. Map of the study area, including the location of Yeonggwang and Wido tidal gauge station (stars).

DEM by stacking a series of waterlines observed under different tidal conditions.

There are several procedures to define the waterline from remotely sensed images, and these can be separated into two methods, namely the automatic approach, and the digitizing method through visual investigation. Due to image noise and the uncertainty associated with the extraction process, the waterlines defined by automatic methods were usually discontinuous, and further modification was required (Liu et al., 2012). On the other hand, human eyes are generally sensitive to edges and boundaries, such as waterlines in satellite images, even though they cannot perform mathematical measurements. Additionally, rational judgment skills provide useful inputs in defining which edges are relevant (Niedermeier et al., 2005). Therefore, the digitizing method through visual investigation is an effective and straightforward procedure, here employed to obtain accurate and reliable waterlines.

Using this approach, a series of waterlines the waterlines of each season were extracted from the satellite images. Then, the summer and winter seasons DEMs (S_DEM and W_DEM, respectively) were generated using the Natural Neighbor interpolation algorithm (Sibson, 1981), based on the extracted summer and winter waterlines. This algorithm finds the closest subset of input samples to a query point and applies weights to them based on proportionate areas to interpolate a value. This method is also known as Sibson or "area-stealing" interpolation. Finally, the seasonal topographic changes were calculated by subtracting W_DEM from S_DEM. In addition, net overall deposition budget also was calculated which use of deposition and erosion area and height of seasonal topographic changes, it can be represented as Eq. (2):

Table 1
List of satellite images used in this study. The images of Landsat TM and ETM+ were acquired during winter and summer seasons in 2003 and 2004 and corresponding tidal heights were measured at the closest tidal gauge stations.

No.	Sensor	Date	Season	Tidal height (cm)	Location
1	Landsat TM	10 DEC. 2003	Winter	110	Gomso Bay
2	Landsat TM	12 FEB. 2004	Winter	205	Gomso Bay
3	Landsat ETM+	16 JAN. 2003	Winter	385	Gomso Bay
4	Landsat ETM+	3 JAN. 2004	Winter	456	Gomso Bay
5	Landsat TM	5 JUL. 2004	Summer	129	Gomso Bay
6	Landsat TM	3 JUN. 2004	Summer	221	Gomso Bay
7	Landsat ETM+	14 AUG. 2004	Summer	320	Gomso Bay
8	Landsat TM	21 SEP. 2003	Summer	406	Gomso Bay
9	Landsat ETM+	29 JUL. 2004	Summer	458	Gomso Bay
10	Landsat TM	10 DEC. 2003	Winter	108	Hampyeong Bay
11	Landsat ETM+	1 FEB. 2003	Winter	183	Hampyeong Bay
12	Landsat ETM+	16 JAN. 2003	Winter	373	Hampyeong Bay
13	Landsat TM	25 FEB. 2003	Winter	467	Hampyeong Bay
14	Landsat TM	5 JUL. 2004	Summer	124	Hampyeong Bay
15	Landsat TM	3 JUN. 2004	Summer	213	Hampyeong Bay
16	Landsat ETM+	14 AUG. 2004	Summer	309	Hampyeong Bay
17	Landsat TM	21 SEP. 2003	Summer	393	Hampyeong Bay
18	Landsat ETM+	27 JUN. 2004	Summer	461	Hampyeong Bay

$$NB = DA \times TC + EA \times TC \quad (2)$$

Where, *NB* is net overall sedimentation budget (unit), *DA* is deposition area (m^2) and *EA* is erosion area (unit) and *TC* is height of seasonal topographic changes (unit: m).

3. Results

Fig. 2 represents the extracted waterlines and DEMs of the tidal flats in Gomso (Fig. 2a and b) and Hampyeong (Fig. 2c and d) Bays by the digitizing through visual investigation method. The DEMs are overlaid by the waterlines during winter and summer seasons drawn in blue and red gradient colors, respectively. The background image corresponds to the NIR band of the Landsat TM satellite image, acquired on December 10, 2003, when the tidal height was around 110 cm. The waterlines in Gomso Bay represent tidal heights ranging from 110 to 456 and 129–458 cm during winter and summer season, respectively, as shown in Fig. 2a and b. Similarly, the waterlines in Hampyeong Bay represent tidal heights ranging from 108 to 467 cm and 124–461 cm during winter and summer season, respectively as shown in Fig. 2c and d. The DEMs were interpolated with a spatial resolution of 0.3 m and the boundary conditions, the maximum and minimum height of the interpolation, were employed from the height ranges of each season.

The accuracy of a DEM yielded by the waterline method largely depends on the accuracy of the waterlines. The average length of the extracted waterlines was about 51,785 and 66,954 m slightly varying depending on tidal heights; the average number of vertices to establish a single waterline was approximately 387 and 581 corresponding to one vertex for every 4 pixels (Tables 2 and 3).

The seasonal topographic variations, i.e., DEM_S minus DEM_W, are shown in Fig. 3 where green and red color represents summer deposition and summer erosion. In this study, summer deposition means that the surface height of summer season is relatively higher (relatively deposited) than that of winter season, while summer erosion represents that the surface height of summer season is relatively lower (relatively eroded) than that of winter season.

For comparison of spatial patterns in Gomso and Hampyeong Bay, the study areas were split into outer, middle and inner part. This separation considers the direction of the formation and the length of bays (Fig. 3 a and b). The interval between sections was ~6 km, each was defined as Gomso_1 (outer), 2 (middle) and 3 (inner) in Gomso Bay (Fig. 3a) whereas the interval of Hampyeong Bay was ~5 km. These were labeled as Hampyeong_1 (outer), Hampyeong_2 (middle) and Hampyeong_3 (inner) (Fig. 3b).

In Gomso Bay, summer deposition was observed moving away from the offshore whereas summer erosion was spatially distributed around the landward direction near the offshore. In overall, the average seasonal topographic variation of the entire bay illustrates that summer deposition was dominant in winter during 2003–2004 year (Table 4). The largest summer deposition was observed in the outer part (Gomso_1) with 32.2 cm; relatively smaller summer deposition was observed in the middle (Gomso_2) and inner (Gomso_3) part of the bay with the average topographic changes of 5.1 and 18.5 cm, respectively.

In Hampyeong Bay, summer deposition was distributed around the main tidal channels. The summer erosion was mainly observed inshore of the most parts of Hampyeong Bay. The spatial average of each section of Hampyeong Bay is listed in the lower part of Table 4. The average seasonal topographic change of Hampyeong_1 was around 1.5 cm representing summer deposition. On the other hand, summer erosion was dominant with the topographic changes of −9.3 cm and −7.2 cm in the middle (Hampyeong_2) and the inner (Hampyeong_3) segment of the bay, respectively.

Fig. 4 shows the quantitative topographic variation in Gomso and Hampyeong Bay. The maximum variation (summer deposition) was spotted in the entrance area in Gomso Bay; the largest summer erosion was observed in the middle and inner part. In Hampyeong Bay, the largest summer deposition was located around the inner southern part of the bay where summer erosion also showed the strong signal in north. The main cause of these local maximum topographic variations are suspected to be the migration of tidal creeks and that main tidal creeks are developed inside bays.

Finally, the net overall sedimentation budget was calculated, using the deposition and erosion area, and height from seasonal topographic changes results. From the results, it is estimated that the net overall sedimentation budget was 6,308,047m3 and −2,210,986 m3 in the Gomso and Hampyeong Bay, respectively.

4. Discussion

The overall average topographic variation of tidal flats in Gomso and Hampyeong Bay was about 18.6 cm and −0.5 cm, respectively.

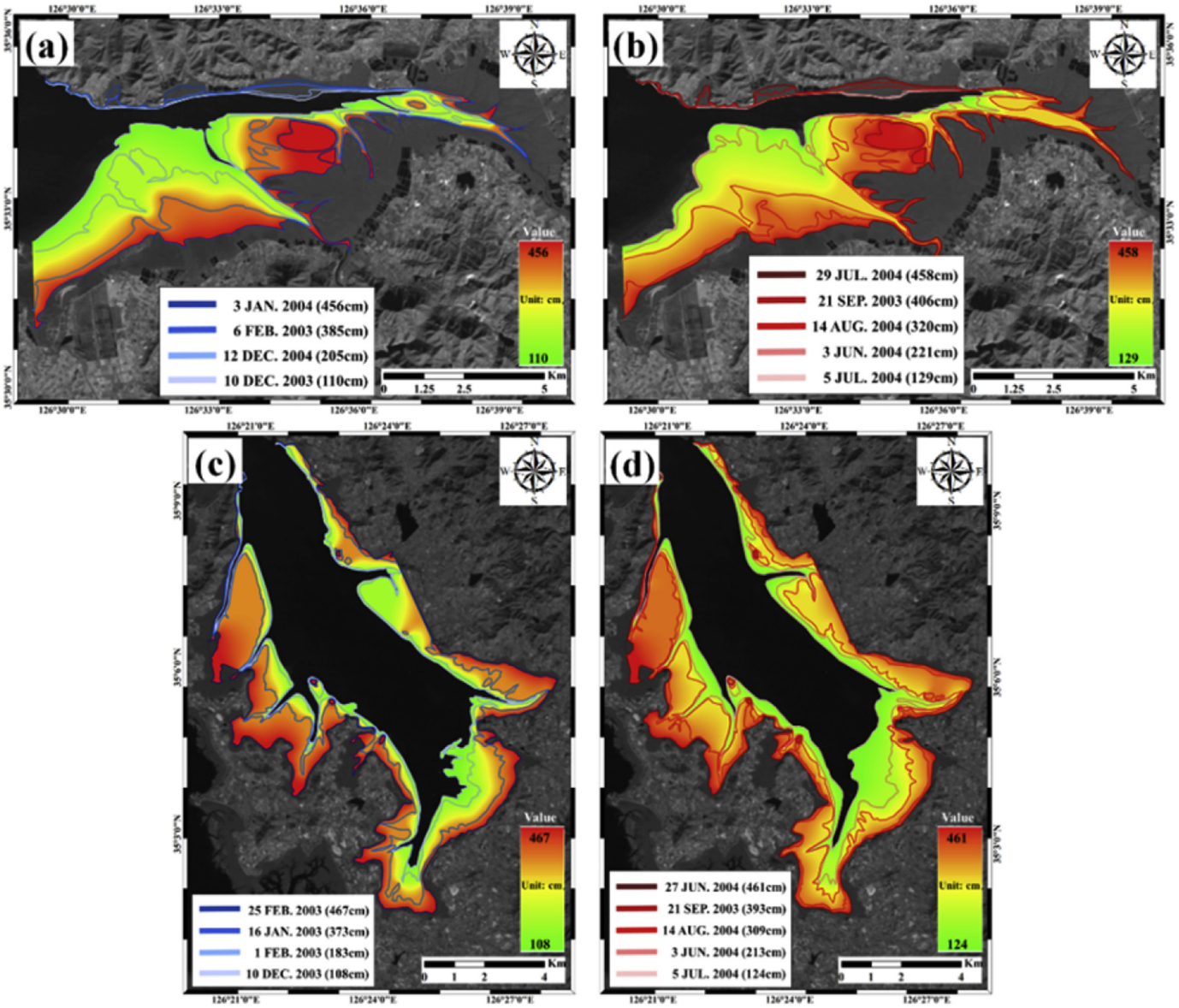

Fig. 2. Generated DEMs of winter and summer seasons overlaid by the extracted waterlines represented in winter (bluish solid lines) and summer (reddish solid lines) in Gomso (a,b) and Hampyeong (c,d) Bay, respectively. (a) W_DEM of Gomso bay; (b) S_DEM of Gomso Bay; (c) W_DEM of Hampyeong bay and (d) S_DEM of Hampyeong bay. (For interpretation of the references to colour in this figure legend, the reader is referred to the web version of this article.)

Table 2
Detailed information about the extracted waterlines in Gomso Bay. The length of each waterline slight varies depending on the tidal height of the acquisition date.

No.	Date	Tidal height (cm)	Location	Waterline length (m)	Vertices	length per vertex (m)
1	10 DEC. 2003	110	Gomso Bay	33,523	173	194
2	12 FEB. 2004	183	Gomso Bay	52,264	388	135
3	16 JAN. 2003	373	Gomso Bay	54,930	442	124
4	3 JAN. 2004	467	Gomso Bay	65,075	447	146
5	5 JUL. 2004	129	Gomso Bay	27,084	115	236
6	3 JUN. 2004	221	Gomso Bay	36,339	310	117
7	14 AUG. 2004	320	Gomso Bay	49,612	230	216
8	21 SEP. 2003	406	Gomso Bay	77,207	708	109
9	29 JUL. 2004	458	Gomso Bay	70,032	669	105
Average				**51,785**	**387**	**134**

Although Gomso and Hampyeong Bay consist of semi-enclosed tidal flats, the seasonal topographic variation in each bay was different during 2003–2004 season; summer deposition was dominant in Gomso Bay whereas summer erosion was dominant in Hampyeong Bay. These results are consistent with previous studies providing field measurements (Alexander et al., 1991; Ryu et al.,

Table 3
Detailed information about the extracted waterlines in Hampyeong Bay. The length of each waterline slight varies depending on the tidal height of the acquisition date.

No.	Date	Tidal height (cm)	Location	Waterline length (m)	Vertices	length per vertex (m)
1	10 DEC. 2003	108	Hampyeong Bay	62,208	406	153
2	1 FEB. 2003	183	Hampyeong Bay	65,987	574	115
3	16 JAN. 2003	373	Hampyeong Bay	79,716	787	101
4	25 FEB. 2003	467	Hampyeong Bay	69,872	744	94
5	5 JUL. 2004	124	Hampyeong Bay	45,292	308	147
6	3 JUN. 2004	213	Hampyeong Bay	67,429	489	138
7	14 AUG. 2004	309	Hampyeong Bay	74,741	683	109
8	21 SEP. 2003	393	Hampyeong Bay	74,133	732	101
9	27 JUN. 2004	461	Hampyeong Bay	63,207	508	124
Average				**66,954**	**581**	**115**

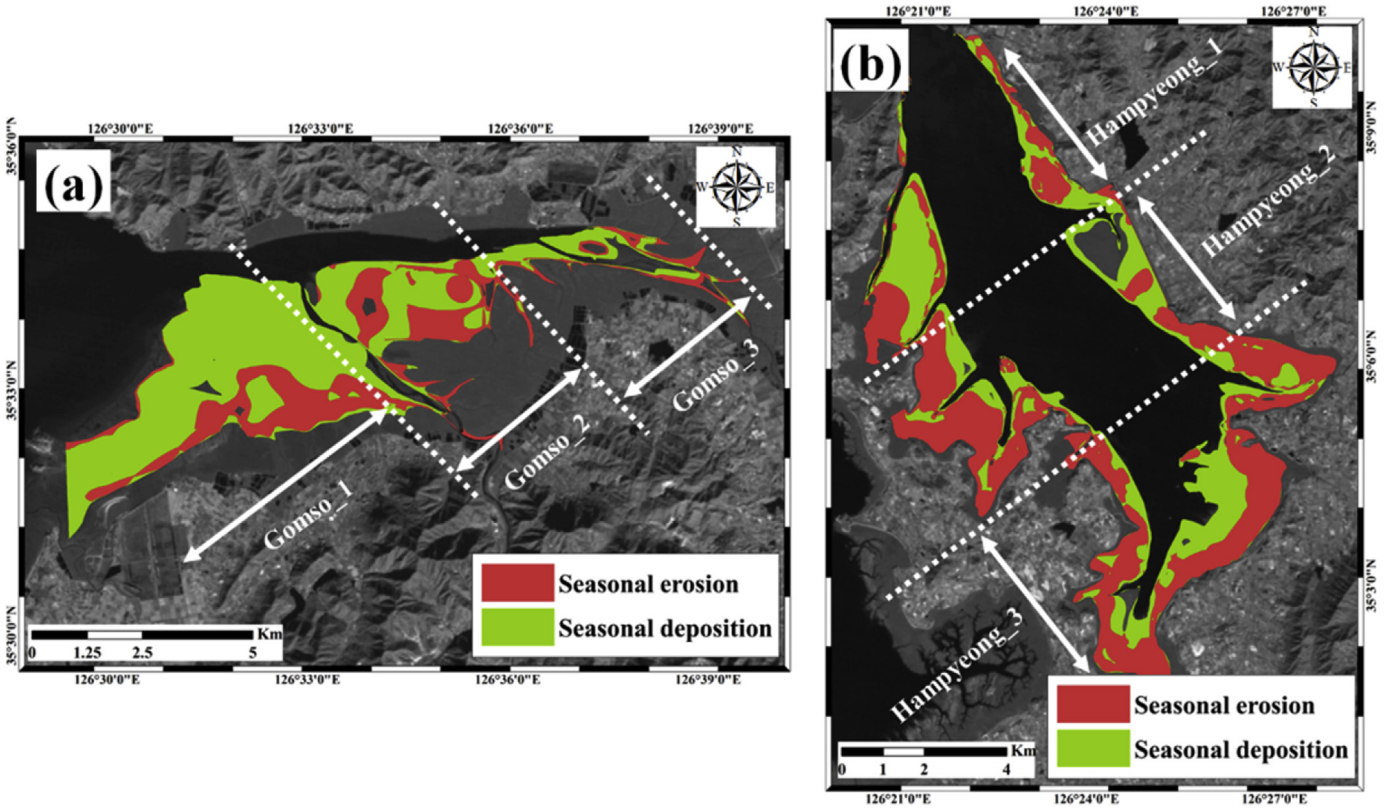

Fig. 3. Spatial distributions of summer deposition and erosion are shown in green and red, respectively. The entire bays are split into 3 sections according to the length and formation shape of each bay. (a) Gomso Bay; (b) Hampyeong Bay. (For interpretation of the references to colour in this figure legend, the reader is referred to the web version of this article.)

1999; Ryu, 2003). Possible sources for this difference are considered to reside in the formation shape and sediment type of the tidal flats. Concerning the formation shape, the tidal flat in the Hampyeong Bay was developed along north-west and south-east directions with a narrow bay mouth. In contrast, the tidal flat in Gomso Bay was developed along the east-west direction with a wide bay entrance. In general, the monsoon is directly associated with wind direction of which blows from the north-west in the winter of the Korea Peninsula. Hampyeong and Gomso Bay have different formation shapes with different directions so that each has divergent influence from the monsoon. The erosion is relatively weaker in Hampyeong Bay of which the south-west main tidal channel diminishes the most of wave energy coming from the north-west and is connected to the bay-mouth of less than 2 km wide. On the other hand, the mouth of Gomso Bay is open towards the west with the width of about 9 km. This relatively large bay-mouth with the right direction is easily exposed to the waves from the north-west direction, influenced by the monsoon, causing the dominant erosion effect. Thus, it was analyzed that the morphology and direction of the bays have strong relation with the monsoon. In this regard, wave, typhoon, and storm events exert comparatively larger influences on the Gomso, whereas

Table 4
Quantitative seasonal topographic changes in Gomso and Hampyeong Bay. The average variation of each section is also listed.

Bay	Seasonal topographic variation (cm)	Overall average seasonal topographic variation (cm)
Gomso_1	32.2	**18.6**
Gomso_2	5.1	
Gomso_3	18.5	
Hampyeong_1	1.5	**−5.0**
Hampyeong_2	−9.3	
Hampyeong_3	−7.2	

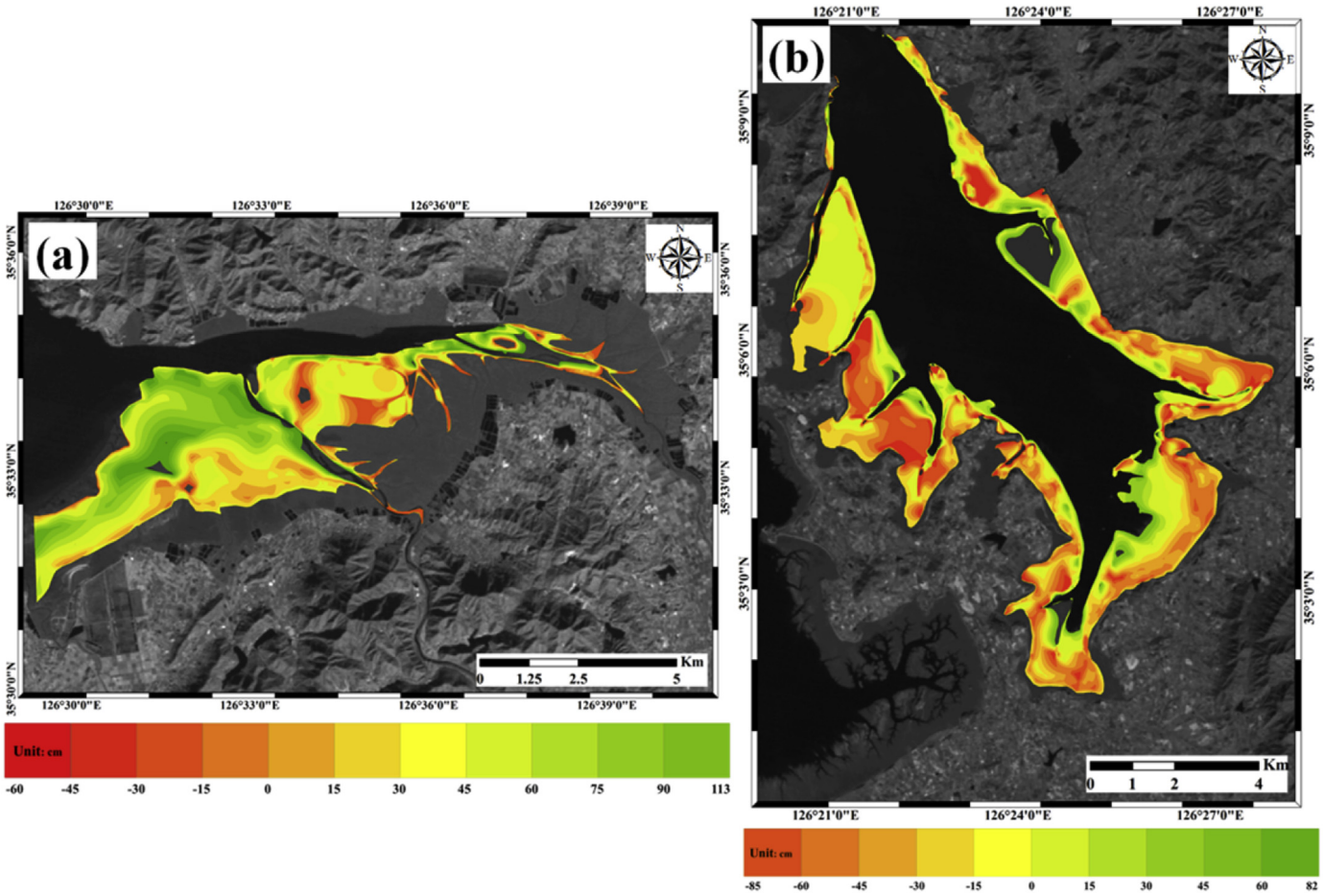

Fig. 4. Quantitative seasonal topographic variations of (a) Gomso Bay and (b) Hampyeong Bay. The maximum summer deposition was spotted near the entrance of Gomso Bay while the largest summer erosion was observed in the middle and inner part. In Hampyeong Bay, the largest summer deposition was located around the inner southern part of the bay.

Hampyeong Bay is well protected from those.

Tidal currents are generally the predominant sedimentary forcing agents in semi-enclosed bay environments, yielding extensive muddy tidal flats with limited sand bar formation, and a typical trend of seawards grain-size coarsening (Alexander et al., 1991; Frey et al., 1989; Postma, 1961; Van Straaten and Kuenen, 1957; Wells et al., 1990). However, Hampyeong Bay rarely follows these characteristics since the bay includes well-developed mixed flats, mud flats and sandy bodies, such as sand bars and cheniers. This unusual seasonal sedimentary pattern in Hampyeong Bay is not only controlled by tidal currents, but also by other factors such as monsoon storms and bay morphology.

This study attempts to estimate the accurate seasonal topographic variations based on the waterline method. Also, the limitations in selecting suitable Landsat datasets were included. First of all, for the waterline method, it is recommended to acquire image data in a short period of time at different tidal heights in order to obtain a good quality of the DEM. However, because of the nature of satellite trajectory assigned to the specified time, the time span of the obtained data corresponding to the various tide became inevitably long. Furthermore, the quality of the data is extremely sensitive to the effect of weather. These factors increase the time span of the data to many years. Therefore, the effort to collect the data in a short time span to reflect the representative topography changes was necessary. In this study, we were able to obtain suitable Landsat images as short as possible during the period from 2003 to 2004.

In general, the sedimentation changes (deposition and erosion) of coastal area are predominantly influenced by the tidal current and the waves' energy and propagation direction. The tidal current and waves' propagation direction are influenced by the bathymetry, coastal features, and winds (Lee et al., 2010), but the bathymetry and coastal features are not significantly changed in short period of time. Thus, the prevailing wind is the most dominant contributor to the generation of tidal current and waves. Because the Korea has monsoon season, the wind direction in winter from northwest to southeast and vice versa in summer, the characteristics of wind direction and strength have distinct in summer and winter. The strong winds can be generated by the wind storm. Most wind storms which were affected by monsoon wind direction were occurred in winter season in Korea (Korea Meteorological Administration, 2003, 2004), significant erosion can be occurred in winter season. Therefore, the characteristics of seasonal topographic variations in Gomso and Hampyeong Bay can be well represented by the DEMs generated in summer and winter.

5. Conclusions

The seasonal topographic variation of major tidal flats in the southern part of the west sea of South Korea were quantitatively estimated by comparing the seasonal topographic differences between summer and winter DEMs derived from the waterline method. These comparisons conclude that summer deposition is the dominant effect in Gomso tidal flats with an average overall seasonal topographic change of 12.8 cm. In contrast, summer erosion is dominant with −5.0 cm topographic variation in Hampyeong Bay. Also, the net overall sedimentation budget was

calculated; it was 6,308,047 m^3 and -2,210,986 m^3 in Gomso and Hampyeong Bay, respectively. Although both Gomso and Hampyeong Bay are classified as semi-enclosed coast tidal flat, the sedimentary facies caused by formation geometry and sediment type led to different topographic changes.

In comparison to previous studies, our quantitative results successfully justified the DEM generation of tidal flats, using the waterline method. In particular, the effective detection of seasonal topographic changes in the western coast of South Korea stresses the significance of this study. However, errors from multi-temporal waterlines and dimensional interpolation must also be taken into consideration in further analysis. This research is the first approach of detecting seasonal topographic variations by the waterline method. Consideration of the seasonal topographic changes is essentially important in detecting more accurate long term topographic changes in the tidal flat. Moreover, influential oceanic forces that can have significant influence on sedimentological processes, such as tidal currents, waves, storms, and typhoons, are expected to provide useful information on short-term topographic variations.

Acknowledgments

This research was supported by the Space Core Technology Development program through the National Research Foundation of Korea funded by the Ministry of Science, ICT and Future Planning (2016M1A3A3A04936872 and 2014M1A3A3A03034799). The Landsat data used in this study are available from the U.S. Geological Survey.

References

Ahn, C., Lee, Y., Yoo, H., Oh, J., 1989. Application of satellite data on geomorphological study of the tidal flats near Keum river estuary. J. Korean Soc. Remote Sens. 5, 2–15.
Alexander, C.R., Nittrouer, C.A., Demaster, D.J., Park, Y.-A., Park, S.-C., 1991. Macrotidal mudflats of the southwestern Korean coast: a model for interpretation of intertidal deposits. J. Sediment. Res. 61.
Allen, J., 2000. Morphodynamics of Holocene salt marshes: a review sketch from the Atlantic and Southern North Sea coasts of Europe. Quat. Sci. Rev. 19, 1155–1231.
Allen, J., Pye, K., 1992. Coastal Saltmarshes: Their Nature and Importance. Salt Marshes, Morphodynamics, Conservation and Engineering Significance. Cambridge University Press, Cambridge, pp. 1–18.
Chang, J., Choi, J., 2001. Tidal-flat sequence controlled by Holocene sea-level rise in Gomso Bay, west coast of Korea. Estuar. Coast. Shelf Sci. 52, 391–399.
Chang, J.H., Choi, J.-Y., 1998. Seasonal accumulation pattern and preservation potential of tidal-flat sediments: Gomso Bay, West Coast of Korea. J. Korean Soc. Oceanogr. 3, 149–157.
Chen, L., Rau, J., 1998. Detection of shoreline changes for tideland areas using multitemporal satellite images. Int. J. Remote Sens. 19, 3383–3397.
Choi, S., Lee, W.-K., Kwak, H., Kim, S.-R., Yoo, S., Choi, H.-A., Park, S., Lim, J.-H., 2011. Vulnerability assessment of forest ecosystem to climate change in Korea using MC1 model (< special issue> multipurpose forest management). J. For. Plan. 16, 149–161.
Cracknell, A., 1999. Remote sensing techniques in estuaries and coastal zones an update. Int. J. Remote Sens. 20, 485–496.
Deronde, B., Houthuys, R., Debruyn, W., Fransaer, D., Lancker, V.V., Henriet, J.-P., 2006. Use of airborne hyperspectral data and laserscan data to study beach morphodynamics along the Belgian coast. J. Coast. Res. 1108–1117.
Frey, R.W., Howard, J.D., Han, S.-J., Park, B.-K., 1989. Sediments and sedimentary sequences on a modern macrotidal flat, Inchon, Korea. J. Sediment. Res. 59.
Gade, M., Alpers, W., Melsheimer, C., Tanck, G., 2008. Classification of sediments on exposed tidal flats in the German Bight using multi-frequency radar data. Remote Sens. Environ. 112, 1603–1613.
Gade, M., Melchionna, S., Stelzer, K., Kohlus, J., 2014. Multi-frequency SAR data help improving the monitoring of intertidal flats on the German North Sea coast. Estuar. Coast. Shelf Sci. 140, 32–42.
Green, E., Mumby, P., Edwards, A., Clark, C., 1996. A review of remote sensing for the assessment and management of tropical coastal resources. Coast. Manag. 24, 1–40.
Greidanus, H., Huising, E., Platschorre, Y., Van Bree, R., Van Halsema, D., Vaessen, E., 1999. Coastal DEMs with cross-track interferometry. In: Geoscience and Remote Sensing Symposium, 1999. IGARSS'99 Proceedings. IEEE 1999 International. IEEE, pp. 2161–2163.
Heygster, G., Dannenberg, J., Notholt, J., 2010. Topographic mapping of the German tidal flats analyzing SAR images with the waterline method. Geosci. Remote Sens. 48, 1019–1030. IEEE Transactions on.
Hoja, D., Lehner, S., Niedermeier, A., Romaneessen, E., 2000. DEM generation from ERS SAR shorelines compared to airborne crosstrack InSAR DEMs in the German Bight. In: Geoscience and Remote Sensing Symposium, 2000. Proceedings. IGARSS 2000. IEEE 2000 International. IEEE, pp. 1889–1891.
Klemas, V., 2011. Beach profiling and LIDAR bathymetry: an overview with case studies. J. Coast. Res. 27, 1019–1028.
Korea Meteorological Administration, 2003. Annual Climatological Report 2003.
Korea Meteorological Administration, 2004. Annual Climatological Report 2005.
Lee, M.O., Lee, J.S., Kim, B.K., Kim, J.K., 2010. Wind effect on tidal currents in the neighborhood of Haeundae beach. J. Korean Soc. Coast. Ocean Eng. 22 (1), 34–46.
Lee, Y.-K., Ryu, J.-H., Choi, J.-K., Soh, J.-G., Eom, J.-A., Won, J.-S., 2011. A Study of decadal sedimentation trend changes by waterline comparisons within the Ganghwa tidal flats initiated by human activities. J. Coast. Res. 27, 857–869.
Li, Z., Heygster, G., Notholt, J., 2014. Intertidal topographic maps and morphological changes in the German Wadden sea between 1996–1999 and 2006–2009 from the waterline method and SAR images, IEEE. J. Sel. Top. Appl. Earth Obs. Remote Sens. 7 (8), 3210–3224.
Liu, Y., Li, M., Cheng, L., Li, F., Chen, K., 2012. Topographic mapping of offshore sandbank tidal flats using the waterline detection method: a case study on the Dongsha Sandbank of Jiangsu Radial Tidal Sand Ridges, China. Mar. Geod. 35, 362–378.
Liu, Y., Li, M., Zhou, M., Yang, K., Mao, L., 2013. Quantitative analysis of the waterline method for topographical mapping of tidal flats: a case study in the Dongsha sandbank, China. Remote Sens. 5 (11), 6138–6158.
Mason, D., Davenport, I., Robinson, G., Flather, R., McCartney, B., 1995. Construction of an inter-tidal digital elevation model by the 'Water-Line'Method. Geophys. Res. Lett. 22, 3187–3190.
Mason, D., Gurney, C., Kennett, M., 2000. Beach topography mapping—a comparision of techniques. J. Coast. Conserv. 6, 113–124.
Mason, D., Hill, D., Davenport, I., Flather, R., Robinson, G., 1997. Improving Inter-tidal Digital Elevation Models Constructed by the Waterline Technique, vol. 414. European Space Agency-Publications-ESA SP, pp. 1079–1082.
Niedermeier, A., Hoja, D., Lehner, S., 2005. Topography and morphodynamics in the German Bight using SAR and optical remote sensing data. Ocean. Dyn. 55, 100–109.
Postma, H., 1961. Transport and accumulation of suspended matter in the Dutch Wadden Sea. Neth. J. Sea Res. 1, 148–190.
Ryu, J.-H., Kim, C.-H., Lee, Y.-K., Won, J.-S., Chun, S.-S., Lee, S., 2008. Detecting the intertidal morphologic change using satellite data. Estuar. Coast. Shelf Sci. 78, 623–632.
Ryu, S.-O., You, H.-S., Lee, J.-D., 1999. Seasonal variation of surface sediments and accumulation rate on the intertidal flats in Hampyong Bay, southwestern coast of Korea. Sea 4, 127–135.
Ryu, S., 2003. Seasonal variation of sedimentary processes in a semi-enclosed bay: Hampyong bay, Korea. Estuar. Coast. Shelf Sci. 56, 481–492.
Sallenger, A., Krabill, W., Swift, R., Brock, J., List, J., Hansen, M., Holman, R., Manizade, S., Sontag, J., Meredith, A., 2003. Evaluation of airborne topographic lidar for quantifying beach changes. J. Coast. Res. 19, 125–133.
Sibson, R., 1981. A brief description of natural neighbour interpolation. Interpret. Multivar. data 21, 21–36.
Stockdonf, H.F., Sallenger Jr., A.H., List, J.H., Holman, R.A., 2002. Estimation of shoreline position and change using airborne topographic lidar data. J. Coast. Res. 502–513.
Van Stokkom, H., Stokman, G., Hovenier, J., 1993. Quantitative use of passive optical remote sensing over coastal and inland water bodies. Int. J. Remote Sens. 14, 541–563.
Van Straaten, L., Kuenen, P.H., 1957. Accumulation of Fine Grained Sediments in the Dutch Waddensea.
Wang, Y.P., Zhang, R., Gao, S., 1999. Velocity variations in salt marsh creeks, Jiangsu, China. J. Coast. Res. 471–477.
Waska, H., Kim, G., 2010. Differences in microphytobenthos and macrofaunal abundances associated with groundwater discharge in the intertidal zone. Mar. Ecol. Prog. Ser. 407, 159–172.
Welch, R., Remillard, M., Alberts, J., 1992. Integration of GPS, remote sensing, and GIS techniques for coastal resource management. Photogramm. Eng. Remote Sens. 58, 1571–1578.
Wells, J.T., Adams, C.E., Park, Y.-A., Frankenberg, E.W., 1990. Morphology, sedimentology and tidal channel processes on a high-tide-range mudflat, west coast of South Korea. Mar. Geol. 95, 111–130.
Wimmer, C., Siegmund, R., Schwabisch, M., Moreira, J., 2000. Generation of high precision DEMs of the Wadden Sea with airborne interferometric SAR. Geosci. Remote Sens. 38, 2234–2245. IEEE Transactions on.
Yoo, H.-R., Bae, I.-H., Ryu, J.-H., Ahn, Y.-H., 2005. A study of the sedimentary environments in the Korean tidal flat using Landsat TM/ETM+, Kompsat EOC, and IKONOS. In: Geoscience and Remote Sensing Symposium, 2005. IGARSS'05. Proceedings. 2005 IEEE International. IEEE, 3 pp.
Zhao, B., Guo, H., Yan, Y., Wang, Q., Li, B., 2008. A simple waterline approach for tidelands using multi-temporal satellite images: a case study in the Yangtze Delta. Estuar. Coast. Shelf Sci. 77, 134–142.